

Linguistic networks uncover grammatical constraints of protein sentences comprised of domain-based words.

Adrian A. Shimpi^{1,2}, Kristen M. Naegle^{1,2,*}

1 Department of Biomedical Engineering, University of Virginia, Charlottesville, VA, 22903

2 Department of Genome Sciences, University of Virginia, Charlottesville, VA, 22903

* Correspondence: kmn4mj@virginia.edu

Abstract

Evolution has developed a set of principles that determine feasible domain combinations analogous to grammar within natural languages. Treating domains as words and proteins as sentences, made up of words, we apply a linguistic approach to represent the human proteome as an n-gram network. Combining this with network theory and application, we explore the functional language and rules of the human proteome. Additionally, we explored subnetwork languages by focusing on reversible post-translational modifications (PTMs) systems that follow a reader-writer-eraser paradigm. We find that PTM systems appear to sample grammar rules near the onset of the system expansion, but then convergently evolve towards similar grammar rules, which stabilize during the post-metazoan switch. For example, reader and writer domains are typically tightly connected through shared n-grams, but eraser domains are almost always loosely or completely disconnected from readers and writers. Additionally, after grammar fixation, domains with verb-like properties, such as writers and erasers, never appear – consistent with the idea of natural grammar that leads to clarity and limits futile enzymatic cycles. Then, given how some cancer fusion genes represent the possibility for the emergence of novel language, we investigate how cancer fusion genes alter the human proteome n-gram network. We find most cancer fusion genes follow existing grammar rules. Collectively, these results suggest that n-gram based analysis of proteomes is a complement to the more direct protein-protein interaction networks. N-grams can capture abstract functional connections in a more fully described manner, limited only by the definition of domains within the proteome and not by the combinatorial challenge of capturing all protein interaction connections.

1 Introduction

2 Domains are modular units of structure and function that enable protein complex formation or translate
3 biochemical information between signaling effectors[1]. About half of the human proteome is comprised
4 of multidomain proteins, where domains help define overall protein functionality through their
5 independent contributions. The combination of domains within a protein, or domain architecture, arises
6 primarily through the shuffling of preexisting domains, rather than the emergence of new domains[2–4].
7 Evolutionary jumps, encoded within the domain architectures of protein families, can predict the
8 acquisition of new protein functions[3, 5]. Changes in domain architectures most commonly occur from
9 the gain or loss of domains from the terminal ends of preexisting proteins[6]. Interestingly, only a small
10 fraction of possible domain combinations are observed, which cannot be described by the random
11 shuffling of domains during genetic recombination events[3, 4, 7], but can be attributed to few domains
12 having multiple domain partners[8, 9]. These observations have motivated the representation of proteins
13 as vectors comprised of their domains for evaluating the evolution of protein families and the complete
14 proteome[3, 5, 10]. Further, these representations have been used to predict the subcellular localization
15 and gene ontology terms for individual proteins[11, 12] demonstrating the breadth of information
16 encoded within overall protein domain architectures.

17 Insights from broad surveys of both protein domain architectures and amino acid sequences suggest
18 that proteins operate with sets of rules akin to grammar within natural languages[10, 13, 14]. However,
19 the development of protein language models often focus on the amino acid sequence to predict the
20 structure, function, and evolution of unresolved proteins or guide novel protein design[13, 15–17].
21 Despite the breadth of information encoded within domain architectures few linguistic approaches have
22 used domains as the fundamental unit of the protein language. Applications that utilize domains as
23 "words" within a protein have shown linguistics can recover protein functionality and evolution across
24 the tree of life independent of known protein interaction networks or signaling pathways[5, 10]. However,
25 these past methods rarely consider the word ordering and word repeats, which likely reflect the
26 evolutionary pressures related to the non-random shuffling of domains and the observation of the
27 predominant modification of domain architectures at the terminal ends[3, 4, 6, 7]. The sequential order
28 can have important consequences on protein functions like modifying the avidity or specificity of
29 catalytic domains like the tyrosine kinase domain[18, 19]. Like natural languages, there are likely
30 constraints on the relative location and combination of certain word types that make up human proteins.
31 For example, catalytic domains might represent verbs and the binding domains they appear with are
32 adverbs, or possibly as the nouns or subject of the sentence that help define the action the verb will have.
33 Certain types of adverbs or the combination of too many verbs without modifying nouns may be
34 prohibited from a language that ultimately needs to be interpreted by the biochemical networks of the
35 cell, while also maintaining sentence clarity (akin to minimizing energy usage).

36 N-gram analysis is a linguistic approach which maintains both the composition and sequential order
37 of words within natural languages and can be adapted to protein domain architectures. By treating
38 individual domains as words and the complete domain architecture as a sentence, n-grams with n
39 domains can be extracted from either single or multiple domain architectures. A 2-gram model has
40 shown that pairwise domain combinations can recapitulate the evolution of proteome complexity[10].
41 The smaller fraction of multidomain proteins in prokaryotes than eukaryotes[20] has limited n-gram
42 analysis to mostly 2-gram models for comparative genomic studies. However, certain 2-3 domain
43 combinations, or supra-domains, are rearranged together as a unit across protein families[21]. If an
44 n-gram model does not extract n-grams longer than these supra-domains, the diversity of feasible domain
45 combinations in a proteome may not be sufficiently recovered.

46 Here, we evaluate n-gram models of various lengths to describe the human proteome. We integrate
47 these models with network analysis techniques to identify protein domains and multidomain n-grams
48 that act as hubs to connect obligate domain families, enabling a simplification of the overall network. An
49 advantage of representing the human proteome as a language-based network is that all proteins have
50 defined domains, unlike networks that rely on protein-protein interactions that have yet to be fully
51 annotated[22, 23]. However, the connections within the network reflect more about the related functional
52 connections amongst key words in the human proteome than it does direct protein-protein interactions.
53 Here, we develop and test n-gram networks at the level of the entire proteome, characterizing the
54 entropic information needed to recover most of the proteome. Next, we applied n-gram analysis to
55 measure the emergent properties of the specific words and languages within reader-write-eraser systems
56 that coordinate post-translational modifications (PTMs). Surprisingly, we find that despite vastly
57 different evolutionary timescales, most reversible PTM-systems convergently evolved to have tight
58 connections between the readers and writers and very loosely, if at all connected, erasers. Looking across
59 evolution, it appears that how PTM systems sampled different word ordering gives a possible measure of
60 the relative time since the appearance of the system and the time at which the language becomes fixed
61 in terms of its grammar rules and composition. We then ask if n-gram based network analysis can lead
62 to novel insights to how cancer gene fusions alter, or not, the functional connections within the proteome.
63 Interestingly, we find that predominantly somatic fusion genes arise with the same characteristics that
64 appear to guide the overall evolution of most multidomain protein architectures[3, 4]. Hence, we find
65 that n-gram linguistic analysis of proteomes is highly useful at making entire proteome-level insights
66 about the functional connections between proteins and systems within cells, along with being useful for
67 subnetwork analysis, such as evaluated in the PTM system.

Results

Generating domain n-gram networks to describe the domain architecture landscape

In order to describe the entire human (or other species) proteome as an n-gram network, we relied on the InterPro database, using our recently developed python-based package CoDIAC[24] to annotate the unique proteome domain and domain architecture (sequential ordering of domains in a protein). The InterPro database[25] consolidates annotations from databases such as Pfam[26], SMART[27], CATH-Gene3D[28] and others into one central database to define domain families. Importantly, InterPro is closely integrated with the UniProt database that serves as a central, comprehensive repository of protein sequences and functions. The result of our access is a controlled vocabulary based on the InterPro IDs of the architecture and the order of domains in proteins within the proteome of interest. For example, the SRC and ABL kinase families have the domain architecture SH3-SH2-Kinase. We then define all possible n-grams within each protein, maintaining the continuous sequence of domains from the N- to C-terminal. For the SRC and ABL family kinases, this includes three 1-grams (SH3, SH2, Kinase), two 2-grams (SH3|SH2, SH2|Kinase), and one 3-gram (SH3|SH2|Kinase).

We applied this n-gram extraction to the entire human proteome, and then broadly surveyed domain architectures to identify highly prevalent domains and n-grams that span multiple protein families. About 95% of the proteome have domain architectures containing up to 10 domains (Fig. 1B, S1A). The two longest domain architectures were for the protein Titin (TTN, UniProt ID: Q8WZ42) at 303 domains and Obscurin with 66 domains (OBSCN, UniProt ID: Q5VST9) (Fig S1A). Given the roughly 5-fold difference between the two largest domain architectures and TTN being an outlier in our protein set, we extracted n-grams with a length up to 66 domains. In total, 44,425 n-grams were extracted from >18000 proteins. The majority of n-grams were found in only one protein (Fig. 1C). Eight out of the top ten most reoccurring domain n-grams were repeats of the Zinc Finger C2H2 type (Znf-C2H2) domain (Fig. S1B). Beyond the highly repetitive Znf-C2H2 domain containing n-grams, the protein kinase domain and the seven transmembrane region of rhodopsin-like G-protein coupled receptors (GPCR_Rhodpsn_7TM) were the only additional 1-grams within the top 10 overall n-grams (Fig. S1B). Given the dominance in overall n-grams due to repetition, we identified additional n-grams that contain domain repeats. We retrieved n-grams with 2 or 3 domain repeats and found n-grams consisting entirely of the EGF-like, Cadherin-like, Fibronectin type 3 (FN3), Ig-subtype 2 (Ig_sub2), or the RNA recognition motif (RRM) domains, which occurred in more than 100 proteins each (Fig. S1C). Only one heterotypic n-gram (an n-gram that contains different domains) existed within the top 10, which contained both the Znf-C2H2 domain and the KRAB (Krueppel-associated box) domain (Fig. S1C). The KRAB domain has been noted to only occur in proteins with Znf-C2H2 domains and acts as a transcriptional repressor[29, 30]. Interestingly, n-grams with repetitive domains occurred within roughly 100-200 proteins except for n-grams containing the Znf-C2H2 domain that occur in about 700 proteins. Further, the KRAB and Znf-C2H2 domain n-gram was also the only multidomain n-gram that was returned when retrieving either 1-grams or heterotypic n-grams (Fig S1D). Interestingly, Znf-C2H2 containing proteins are one of the largest classes of transcription factors and Znf-C2H2 domain mediates DNA interactions by recognizing 3 or more bases to create a diverse range of recognition motifs[31, 32]. However, while the Znf-C2H2 domain was the smallest of the domains identified in the top n-grams (Fig. S1E), other small domains like the homeobox domain (HD) and Znf-RING domains were not found in large protein families with highly repetitive copies of each domain. Collectively, these results establish the diversity of domain n-grams that exist across the proteome along with helping identify obligate grammar structures (such as the KRAB|Znf-C2H2|Znf-C2H2 3-gram). However, these results highlight that certain protein families, such as the Znf-C2H2 containing proteins, dominate n-gram counting metrics and may obscure the importance of other critical domain families.

Given that n-grams are structured units of language, we can consider n-grams that share common words to have a connection between the individual n-grams, which represents a functional property that determines feasible domain locations and combinations. Thus, we assembled the n-grams of the complete proteome as a network where nodes represent individual n-grams (e.g. SH2, SH3|SH2, or

119 KRAB|Znf-C2H2), and edges designate parent-child relationships where shorter n-grams are found
120 within the longer n-grams (Fig. 1D). For example, if we consider the SH3|SH2 2-gram found within the
121 SRC and ABL kinase family architecture, it will be connected directly to the SH2 and SH3 1-grams, and
122 the SH3|SH2|Kinase 3-gram. We extended this to the 44,245 n-grams we extracted from the proteome to
123 construct a complete n-gram network (Fig. 1D). We then used gross topographical network features, like
124 the number of connected components, to identify n-gram families that share a common set of words. The
125 n-gram network of the proteome contained 1345 connected components and 700 isolates, which represent
126 domains only found on their own across proteins (Fig. S2A). Most non-isolate connected components
127 represented 5 or less proteins, while the largest connected component represented 9937 proteins (Fig.
128 1E). Given that only a small number of domains have a diverse number of domain partners[8], and whole
129 protein families may be represented within individual connected components of the n-gram network, we
130 determined how integrating a node collapsing step within the domain n-gram network construction alters
131 the overall network topology. By collapse groups of n-grams that fully represent the same set of proteins
132 we can reduce the redundancy of information encoded by each node, and further identify n-grams that
133 represent distinct grammar structures (Fig. 1F). The collapsed network (Fig. 1G) increased the number
134 of isolates to 1106 nodes with most representing n-grams of length 5 or less, but one isolate represents an
135 n-gram family containing 14 domains (Fig. S2). Altogether, this suggests that the collapsed n-gram
136 network maintains connections that represent non-redundant grammar structures, which can then be
137 used to explore the rules within the human proteome.

138 Next, we asked if we can use node-specific metrics to identify critical n-grams of the network. For
139 this, we calculate: 1) the degree centrality – to identify the domains or domain combinations with a
140 diverse set of domain partners, and 2) the betweenness centrality – to identify domain n-grams that
141 connect n-gram families by laying on the shortest path between individual nodes. Using the largest
142 connected component, which represents the most proteins within the proteome, we showcase how these
143 centrality measurements can identify important domain n-grams within the subnetwork. For each
144 n-gram, the degree and betweenness centrality was calculated and shows that a small fraction of n-grams
145 have high values (>0.01) for each metric (Fig. 1H). Exploring the relationship between each centrality
146 measurement (Fig. 1I), we can identify which n-grams act as hubs to connect other n-gram families
147 within the network, and thus represent words with a diverse set of grammar contexts or functions.
148 N-grams with high degree and betweenness centrality values, such as the protein kinase, EGF-like, and
149 Znf-C2H2 domains, have a diverse set of domain partners that demonstrate their flexibility in generating
150 word structures that maintain clear functionality. However, n-grams with only high degree centrality
151 values can represent domain combinations that have several partners but only connect a distinct n-gram
152 family (e.g. highly repetitive domain n-grams that only link to other repetitive n-grams). If an n-gram
153 has a high betweenness centrality but low degree centrality, like the GPCR_Rhodpsn_7TM domain,
154 then it likely acts as a connection between a small fraction of other n-grams to the rest of the network.
155 Even if the individual n-gram is highly prevalent across the proteome, it is highly constrained in what
156 are considered feasible domain partners. This category of n-grams can represent grammar structures that
157 rarely require modifiers to define their action. Altogether, our results demonstrate how an n-gram
158 network can be used to explore the rules of the protein language, and can find abstract connections
159 which maintain protein functionality.

160 **Characterizing the information content and network topology of different** 161 **n-gram length models**

162 Since prior studies used 2-gram models to study domain architectures[3, 8, 10], we set out to evaluate
163 how different n-gram lengths alter the grammar structures of the protein language, which are captured
164 within the topography of the n-gram networks. Importantly, we had found that more than 100 n-gram
165 families comprised of 5 to 14 domains can be collapsed as isolates in the n-gram network (Fig. 1, S2),
166 which suggests 2-gram models may overlook the contributions of supradomains in defining the
167 connections that determine protein functionality[21]. We extracted n-grams ranging from 2-grams up to
168 15-grams, and constructed n-gram networks. Thus, the 3-gram model contained 1-,2-, and 3-grams, while

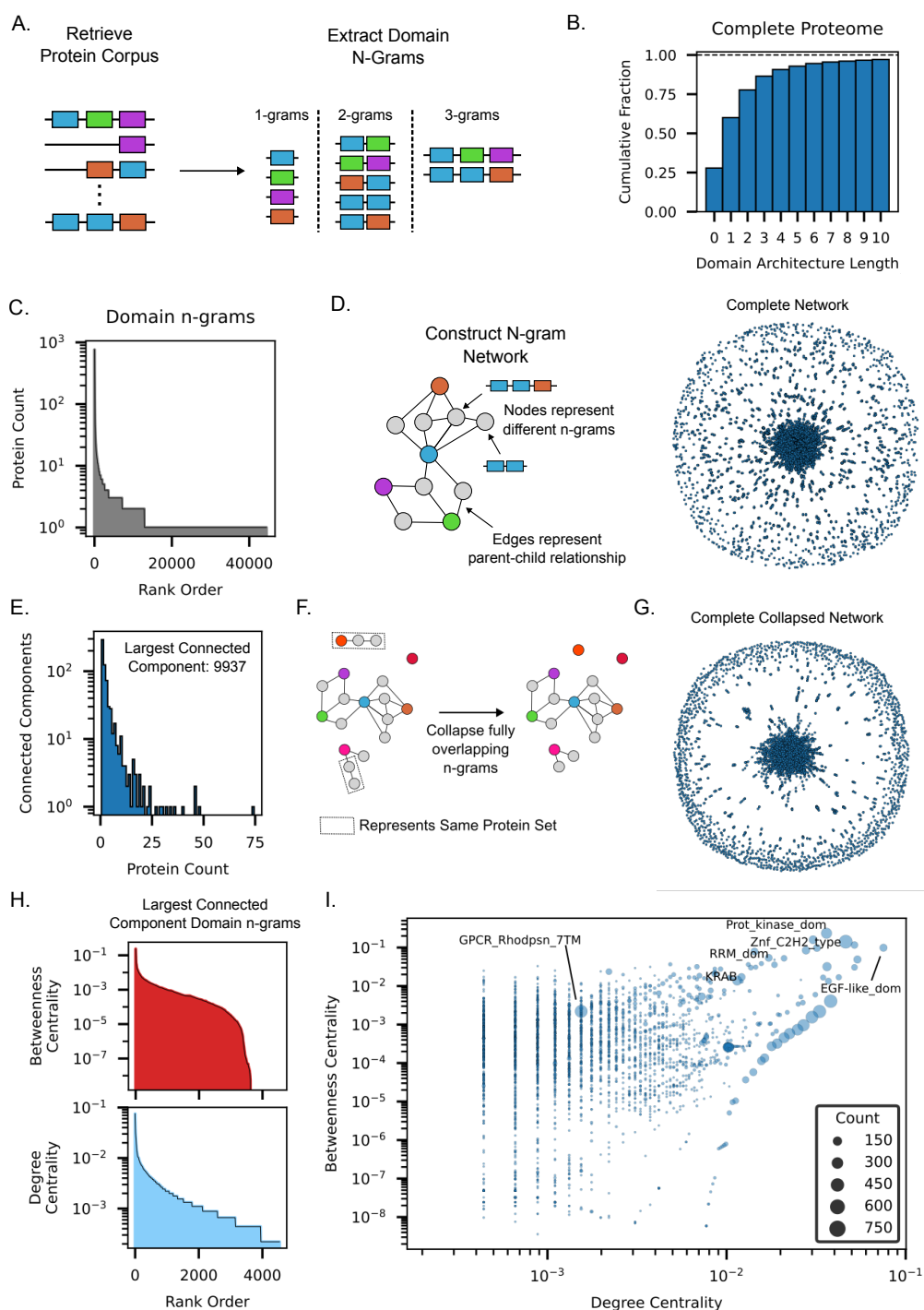


Figure 1. Human proteome n-gram network characterization. A) Overview of extracting n-grams of length n from a collection of protein domain architectures. B) The cumulative distribution of domain architecture lengths across all proteins in the human proteome. C) The number of proteins for each 44,425 domain n-grams. D) The schematic (left) of how the n-gram network was constructed with individual n-grams as nodes within the network and edges representing parent-child relationships where a shorter n-gram is found in a longer n-grams. The actual n-gram network of the complete proteome (right). E) The number of proteins represented for each connected component except the largest connected component which has 9937 proteins. F) Schematic of collapsing n-grams that which fully represent the same set of proteins. G) The collapsed n-gram network of the human proteome. H) Network centrality measurements for each node in the largest connected component of the collapsed n-gram network in rank order. I) The relationship of each centrality measurement with each other and marker size representing the protein count of each n-gram.

169 the 5-gram model contained all those n-grams plus 4- and 5-grams. We measured the entropy of each
170 network model to understand broad changes through emergence or modification of grammatical rules as
171 longer n-grams are included. We compared these entropy values to the natural distribution of domains
172 represented by 1-grams alone, to calculate the relative information gain for each n-gram model, and
173 relative to the full network model. A large information gain of 2 bits occurs with the 2-gram model,
174 however gains became more modest as longer n-grams were included in each model's corpus. The 5-, 10-,
175 and 15-gram models had information gains of 3.77, 4.56, and 4.85 bits respectively, which correspond to
176 71%, 85%, and 91% of the information captured in the full, collapsed n-gram model (Fig. 2A). Using the
177 n-gram networks for the 2-, 5-, 10-, and 15-gram models (Fig 2B), we find most isolates from the original
178 n-gram model were retained across each model. However, the 2-gram and 5-gram models also generated
179 771 and 28 additional isolates respectively (Fig 2C), which suggests that the n-gram families that
180 represent the same set of proteins are being spread across multiple nodes. We next analyzed the changes
181 in non-isolate connected components, and found the 2-gram model only recapitulated half of the existing
182 components in their entirety, and split 16 components into two or more additional components.
183 Meanwhile, the 5-gram split 2 connected components and the 10- and 15-gram models only truncated
184 the connected components by removing nodes associated with longer n-grams (Fig 2D). The 15-gram
185 model only truncated the largest connected component. We calculated the relative entropy of each model
186 to the complete n-gram model to determine the divergence of the n-gram probability distribution, and
187 thus the information content, within each individual model. Like the network changes, the 2-gram model
188 exhibit the highest relative entropy (i.e. largest difference), while the 5-, 10-, and 15-gram models had
189 relative entropy values less than 0.5 bits. Collectively, our results suggest that a 2-gram model is
190 insufficient to accurately recapitulate the diversity of domain n-grams while representing the same set of
191 proteins across different 2-grams. However, n-gram models that include up to 15 domains within an
192 individual n-gram can recapture most of the diversity, but will lose information related to longer n-grams
193 found in roughly 5% of the proteome. However, we observed relatively minimal gains in information
194 content and minimal changes in network topology between 10- and 15-gram models. Thus, for
195 representing the human proteome, we selected a 10-gram model, which appears to be a nice tradeoff
196 between maximizing the information encoded within protein domain architectures and complexity.

197 **Domain modules within reversible PTM systems infrequently share n-grams.**

198 Given that we have established a representation of domain architectures for the entire proteome, we
199 wanted to explore the insights that can be generated from n-gram networks constructed for individual
200 signaling subnetworks, like the phosphorylation system. Phosphorylation is found across many biological
201 processes[33], and is suggested to have developed because the biochemical properties of phosphate groups
202 allow it to be rapidly and readily reversible[34]. This diversity of biological functions can also help
203 explain why the kinase domain is one of the critical n-grams within the complete proteome n-gram
204 network. Signal transduction pathways mediated by phosphorylation are tightly controlled by a three
205 module system which operates under a reader-writer-eraser paradigm. For example, the pTyr machinery
206 consists of the Tyr kinase (writer), Tyr phosphatase (PTP, eraser), SH2 and PTB (readers) domains.
207 Kinases families fall under two broad families: the pTyr and pSer/Thr. However, the pTyr system is
208 considered to be evolutionarily newer having evolved near the origins of metazoan species[35, 36].
209 Unfortunately, the transient nature of phosphorylation and the relatively low affinity of reader domains
210 have made protein-protein interaction network definition especially challenging. To evaluate if linguistic
211 approaches can identify unique characteristics that differ between the two systems, we generated n-gram
212 networks on the components of each phosphorylation system separately (domains and classification in
213 Table S1). Specifically, we generated two n-gram networks for each system, one which contains the
214 complete n-gram corpus, and one with n-grams that only contain at least one of the domains of the PTM
215 system (PTM System Domain Focused). By analyzing the PTM System Domain Focused networks, we
216 can study broad differences in the grammar of system, and how it constrains the combinations of
217 different word types represented by each domain to modulate the overall system. The pTyr system
218 generated a complete connected graph (i.e. a single connected component), while the pSer/Thr system
219 had multiple connected components with n-grams containing the phosphatase (eraser), 14-3-3 (reader),

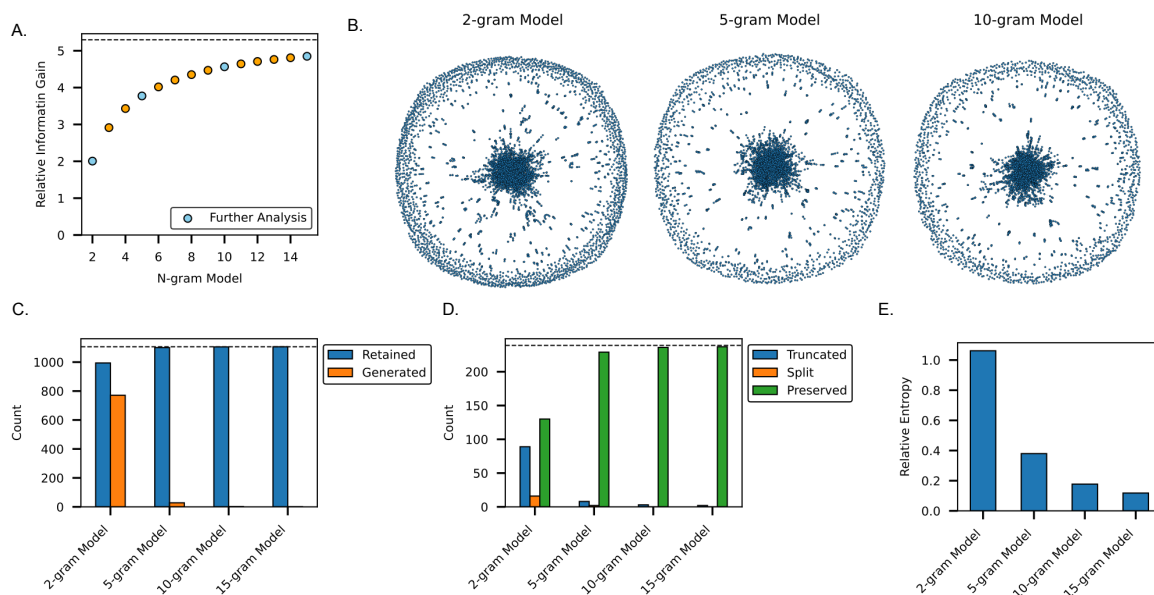


Figure 2. Comparison of different n-gram length models. A) Information gain of different n-gram models relative to a unigram model. B) The n-gram networks of the specified n-gram models. C) The number of isolates generated or retained in each individual n-gram model. D) The number of connected components that were either truncated, split, or fully preserved. E) The relative entropy of each n-gram model to the complete proteome model.

220 or MH2 (reader) domains as individual, disconnected nodes from the rest of pSer/Thr machinery (Fig.
 221 3A). Comparing the complete versus PTM System Domain Focused n-gram networks of the pTyr system
 222 highlighted that only the erasers PTPN6 and PTPN11 with the domain architecture SH2|SH2|PTP use
 223 other pTyr regulatory domains. Meanwhile, the SH2 and Tyr Kinase domains share multiple n-grams
 224 supporting findings that SH2 domains modulate kinase processivity[19, 37]. Within the PTM system
 225 domain focused network of the pSer/Thr system only the FHA domain was directly connected to
 226 Ser/Thr-kinase domain subnetwork (Fig. 3A). Collectively, these results suggest a common set of rules
 227 between the two systems, which includes that eraser domains rarely if at all use the other system
 228 components to modify their function.

229 To determine if the network topologies of the pTyr or pSer/Thr systems were characteristic of other
 230 reversible PTM systems that share the reader-writer-eraser paradigm, we generated networks for the
 231 acetylation, methylation, and ubiquitin systems. From these networks, we found they more closely
 232 resembled the pSer/Thr system with multiple connected components (Fig. 3B, S3A). However, the
 233 methylation system had n-grams with JmjC eraser domains connected to the rest of the network within
 234 the PTM domain focused network, and the DOT writer domains were isolated within both networks
 235 (Fig. S3A). Notably, the PTM System Domain Focused n-gram networks showed each PTM system the
 236 eraser domains are rarely found within the n-grams that contain other system components. To determine
 237 if the PTM System Domain Focused networks were sufficient to recapture the information within the
 238 complete n-gram networks, we calculated the relative entropy between the two models, and found that
 239 the domain focused networks encode similar n-gram distributions across each system (Fig. S3B).

240 Collectively, these results suggest these PTM systems have developed a common set of grammatical rules
 241 that determine the feasible domain combinations to maintain biochemical functions. Interestingly, these
 242 rules suggest that eraser domains do not require additional domains of the system to modify their
 243 activity. Thus reader domains that act as "adverbs" to modify activity of the writer domains, rarely are
 244 used to modulate erasers. Additionally, these networks suggest a constraint that the catalytic domains -
 245 writers and erasers - that act as "verbs" must be on separate proteins that likely prevents inefficient and
 246 futile processing of the PTMs.

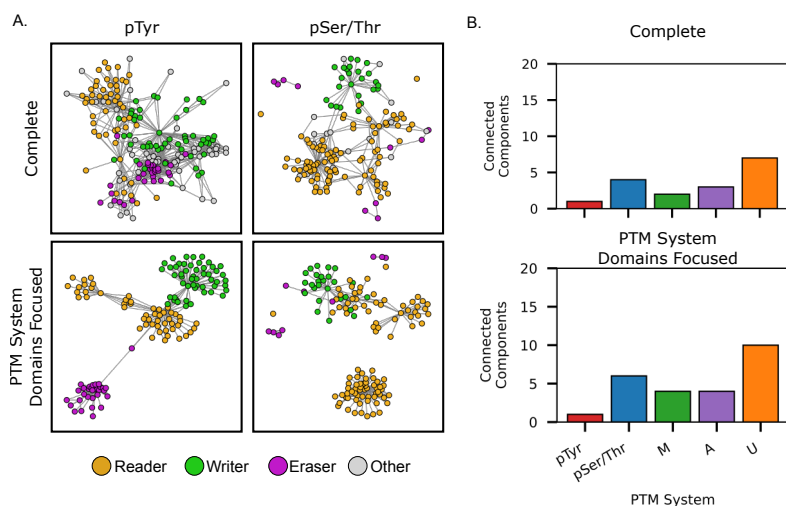


Figure 3. Characterizing the n-gram networks or reversible PTM systems. A) N-gram networks for the phosphotyrosine (pTyr) or phosphoserine/threonine (pSer/Thr) machinery. The top row contains all possible domain n-grams to represent a complete network representation, while the bottom row has n-grams that must contain individual components of the machinery. With the PTM System Domain Focused networks any node which represents both a reader and writer/eraser domain will be colored based on writer/eraser colors. B) The number of connected components for both the phosphorylation systems and additional reversible PTM systems which operate under a reader-writer-eraser paradigm. M: methylation, A: Acetylation, Ub: Ubiquitination

247 Characterizing the evolution of the phosphorylation domain modules.

248 Since the pTyr n-gram networks was the only PTM system that could be represented as a complete
 249 graphs and it is considered one of the most recently evolved PTM systems[35, 36], we wanted to
 250 determine if the n-gram network topology had evolved over time and could reflect the evolutionary age of
 251 the system. We retrieved both the pTyr and pSer/Thr systems from 20 species starting from
 252 *Saccharomyces cerevisiae*, which contains a single proto-SH2 domain and three PTP domains[35] (Fig.
 253 S4). Assembling the n-gram networks for each species, we observe a rapid expansion of both the n-grams
 254 and edges between n-grams for the pTyr system but not the pSer/Thr system (Fig. 4A, S7, S8). The
 255 emergence of metazoans led to the stabilization of the pTyr n-gram network, and is reflected in the
 256 number of connected components and the relative distributions of individual domains (Fig. 4A,B, S4).
 257 For the pSer/Thr system network topology, the separated Ser/Thr phosphatase subnetwork was
 258 established early and few changes in the distribution of individual domains (Fig. 4A,B, S5). These
 259 observations were further supported by using relative entropy to compare the n-gram distributions for
 260 each species to a network generated from all species (Fig. 4C). The relative entropy for the pSer/Thr
 261 networks were lower to begin with in most pre-metazoan species, which reflects the increased similarity
 262 index of the n-grams found within the pSer/Thr network for these species (Fig. S6). Interestingly, these
 263 results suggest a potential convergence of n-grams in both systems during the evolution of vertebrates
 264 within our queried species. However, the individual species networks show an interesting evolution of the
 265 PTM system, which is not readily observed when using the number of individual domains to study the
 266 system evolution alone. The pTyr network of the pre-metazoan species *Capsaspora owczarzaki* and
 267 *Monosiga brevicollis* had several n-grams that connect the PTP domain to the rest of the network that
 268 are lost within metazoans. However, once processes advantageous to metazoans evolved, these n-grams,
 269 with the exception of the SH2|SH2|PTP architecture, were lost. Interestingly, these involved connections
 270 between both catalytic domains, but the only metazoan species where a connection remained was in
 271 *Nematostella vectensis*, which is one of earliest metazoans included in our analysis. This suggests during
 272 this evolutionary period representing the transition to metazoans, species were sampling several
 273 configurations of the network during the rapid pTyr system expansion. However, the pTyr system

274 converged to the similar set of grammatical rules as the other PTM systems, where eraser domains are
275 loosely connected to the rest of the network, and domains with opposing verb actions are not found
276 within the same protein.

277 Using n-gram networks to study gene fusion domain architectures.

278 While advantageous domain architectures have been selected for throughout evolution, selective pressures
279 during the development and progression of cancer present new opportunities for the exploration of new
280 grammatical structures. In particular, the development of cancer fusion genes represents one avenue for
281 generating novel architectures by forming chimeric proteins from genes with disparate functions. For
282 example, the FGFR3-TACC3 fusion gene combines the kinase domain from FGFR3, a receptor Tyr
283 kinase, with the TACC domain (a coiled coil domain) from TACC3, a protein involved in the
284 organization of microtubules during mitosis to form a constitutively active FGFR variant[38]. Relative to
285 the complete n-gram network, gene fusions can generate domain architecture that relate to the gross
286 topology of the n-gram network in three different fashions: 1) the fusion n-gram already exists within the
287 network, and leads to no change, as seen with STK11-TYK2 fusion gene, which retains only the two
288 kinase domains from TYK2 (referred to as no change), 2) a novel domain architecture is generated,
289 which uses domains that share a common domain or n-gram partner to shorten the network path and
290 reinforce an existing connected component, as seen with the BCR-ABL1 fusion gene (referred to as
291 reinforcement), or 3) the novel domain architecture connects domains that do not share any common
292 domain partners and thus only creates articulation points to bridge connected components like the
293 FGFR3-TACC3 fusion (Fig 5A) (referred to as connected components). To investigate the nature and
294 extent of how cancer gene fusions alter n-gram networks, we retrieved gene fusions identified in patients
295 from 20 study cohorts within the Cancer Genome Atlas (TCGA) from the ChimerDB[39]. We limited
296 fusions to those mapped to the current human genome build (hg38) and result in in-frame fusions.
297 Predicted domain architectures were generated by mapping genomic breakpoint information to the
298 protein coding sequence, and identifying the domains being donated from each parent gene (Fig. S9).
299 Across 20 cancer types, at least 40% of all unique fusion gene domain architectures do not create a novel
300 domain architecture with the exceptions of Acute Myeloid Leukemia (LAML) and Testicular Germ Cell
301 Tumors (TGCT). However, for both of these cancers, fewer than 50 fusion genes were identified in their
302 respective studies and resulted in less than 20 unique domain architectures (Fig. 5B). Meanwhile, most
303 of the novel domain architectures reinforced existing domain connections (20-30%), and only 10% of all
304 fusions bridge connected components within the n-gram network (Fig. 5B). The low degree of novel
305 connected components across pancancer gene fusions, suggests that fusion sampling and evolutionary
306 pressures during tumor progression rarely expand the proteome to generate proteins that span disparate
307 functions. However, given the novelty of those fusions that do create new connections, we evaluated
308 whether these fusions represent highly advantageous grammatical structures, which encourage a
309 widespread development across multiple cancers. For each fusion gene, we retrieved their impact on the
310 n-gram network, and then determined whether they were a recurrent fusion across multiple cancer types
311 or within a single cancer. For example, the FGFR3-TACC3 fusion is highly recurrent across multiple
312 cancers[38] and represents a fusion that bridge connected components within the n-gram network.
313 Meanwhile, the TMPRSS2-ERG fusion is highly recurrent within prostate cancer[40], and does not alter
314 the n-gram network. Comparing the n-gram network effects by novel domain architectures generated by
315 these and singleton gene fusions, which have only been identified in one patient, we found irrespective of
316 their recurrent status each group of gene fusions primarily reinforce existing domain combinations (Fig.
317 5C). Altogether, these results suggest that the domain architectures of gene fusions still adhere to the
318 same grammatical rules that were established for domain architectures within the complete proteome.

319 Having established that gene fusions do not readily expand the proteome, we next sought to
320 determine if the few fusions that do connect disparate n-gram families impact patient survival. We
321 stratified patients based on the network impact of their the predicted protein domain architecture of
322 their gene fusion, and if a patient had multiple gene fusions. A pan-cancer, univariate analysis suggested
323 that only patients with gene fusions that reinforce existing domain connections or had multiple fusions
324 were predicted to have worse overall survival (Fig. S10). However, for individual cancer cohorts, the

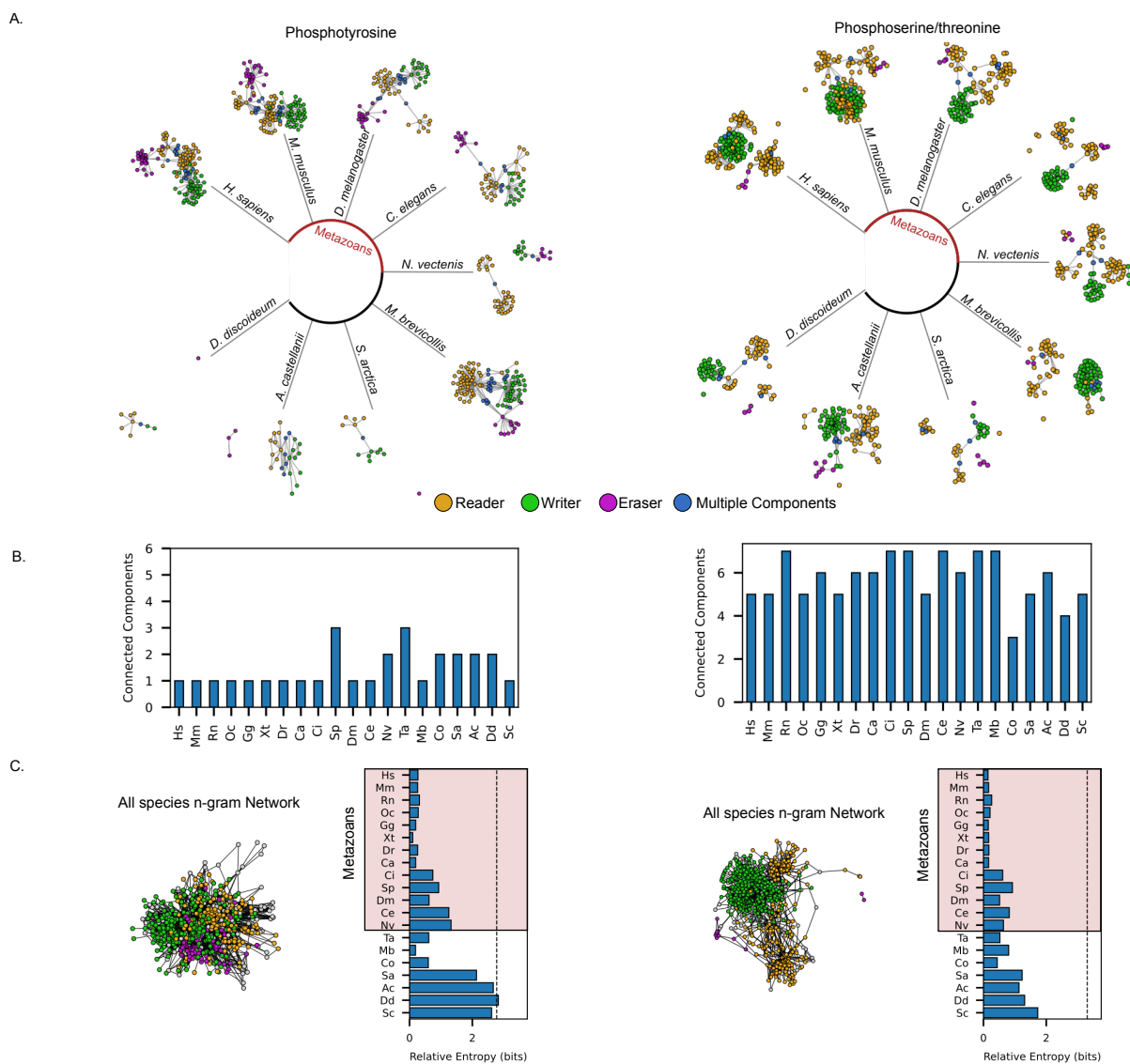


Figure 4. The evolution of the protein domain architectures of the pTyr and pSer/Thr systems. A) Complete n-gram networks of the phosphotyrosine (left) or phosphoserine/threonine (right) systems for species ranging from *Dictyostelium discoideum* to humans. B) The number of connected components for each species phosphorylation system. C) The complete n-gram network containing all n-grams across all queried species and the relative entropy for each species compared to the all species network. Hs: *Homo sapiens*, Ms: *Mus musculus*, Rn: *Rattus norvegicus*, Oc: *Oryctolagus cuniculus*, Gg: *Gallus gallus*, Xt: *Xenopus tropicalis*, Dr: *Danio rerio*, Ca: *Carassius auratus*, Sp: *Strongylocentrotus purpuratus*, Dm: *Drosophila melanogaster*, Ce: *Caenorhabditis elegans*, Nv: *Nematostella vectensis*, Ta: *Trichoplax adhaerens*, Mb: *Monosiga brevicollis*, Co: *Capsaspora owczarzaki*, Sa: *Sphaeroforma arctica*, Ac: *Acanthamoeba castellanii*, Dd: *Dictyostelium discoideum*, Sc: *Saccharomyces cerevisiae*

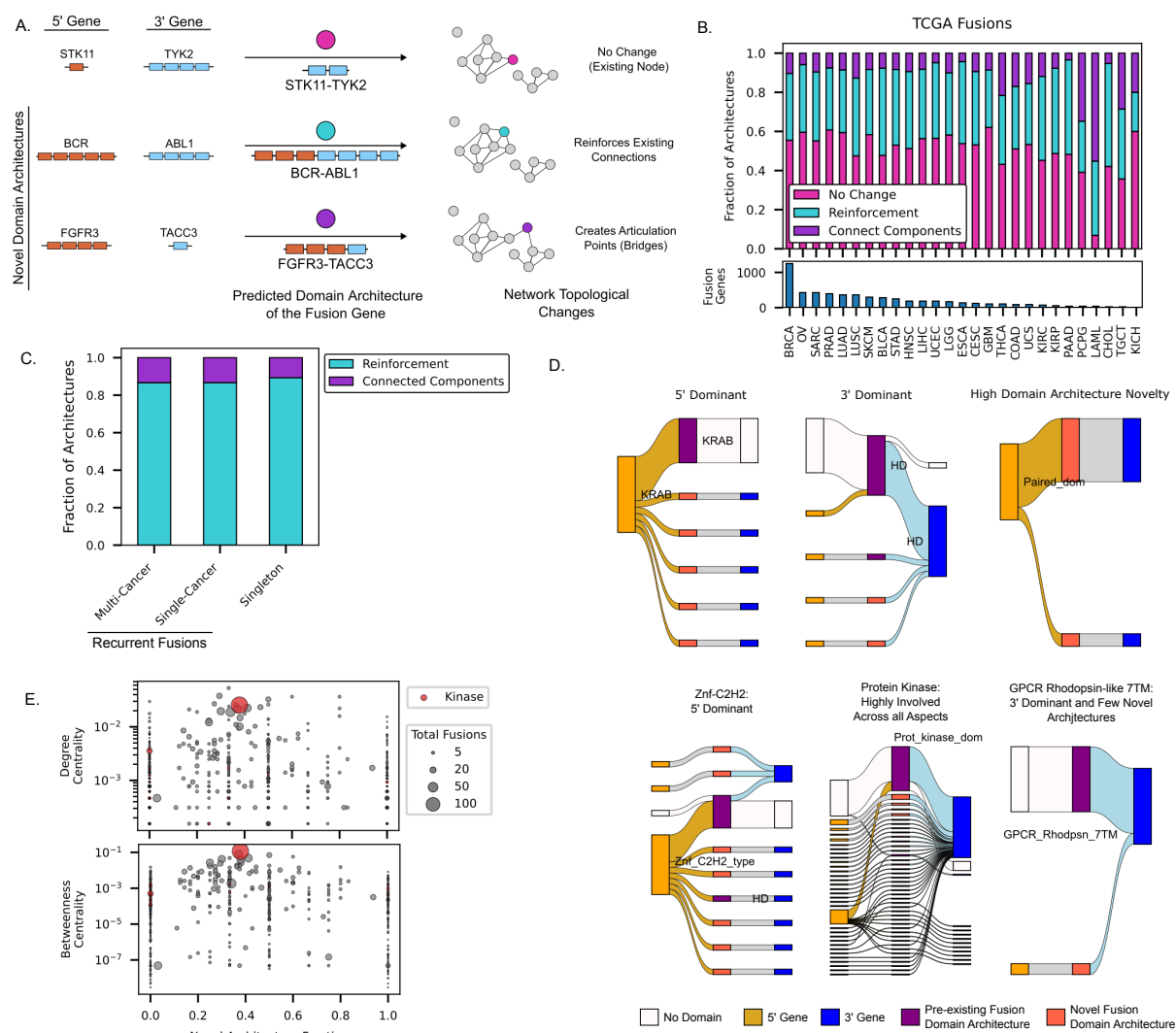


Figure 5. Characterizing predicted protein domain architectures of cancer gene fusions.

A) Schematic of the possible changes to the n-gram network caused by individual fusion genes with example fusion genes are predicted domain architectures. For novel domain architectures these can either reinforce existing connected components or reduce the number of connected components. B) The fractional distribution of fusion gene impacts on the n-gram network (top) and the total number of fusion genes (bottom) retrieved for each TCGA study cohort. C) The distribution of architecture n-gram network impacts for recurrent or singleton fusions within either multiple or single cancer. D) Representative Sankey diagrams of select protein domains that exhibit 5'/3' donation propensity and/or generation of novel domain architectures, and diagrams for the top 3 most prevalent domains across the human proteome. E) Network centrality measurements relative to the fraction of novel domain architectures individual domain n-grams generate. N-grams which contain the protein kinase domain are highlighted in red.

325 presence of gene fusions generally did not predict worse patient survival, except for seven cancers (Fig.
326 S11). Further, stratification by network impacts of gene fusions, and excluding patients with multiple
327 fusions, showed most cancers did not have significant changes in patient survival. However, three cancer
328 cohorts had significantly worse patient survival based on fusion gene stratification, but each cohort had
329 less than 25 patients (5-10% of the patient population) with a single fusion gene limiting the conclusions
330 that can be made on changes in survival probabilities by the n-gram network categories (Fig. S12).
331 Together, these results corroborate that gene fusions are relatively rare events compared to somatic point
332 mutations[41–43]. Further, our results suggest that while gene fusions can identify therapeutic
333 candidates[40, 44], they may not be bona fide biomarkers to predict patient survival, and can even
334 represent passenger mutations[45].

335 Given that our results have established that n-gram networks can highlight broad descriptions of the
336 rules guiding domain architecture development, we constructed an n-gram network on the gene fusions
337 and analyzed the domain architectures of the parent genes. Similar to the natural proteome, most parent
338 genes have domain architectures with two or fewer domains (Fig. S13A). Extracting the individual
339 n-grams donated by the parent genes and the final fusion architecture, we generated a new n-gram
340 network that tracked whether an n-gram was from a parent gene or the final fusion. Thus, if a kinase
341 domain was donated from the 3' fusion gene (e.g. with TYK2) it would be a separate node in the
342 network than a kinase domain that represents the fusion gene (e.g. the complete STK11-TYK2 fusion).
343 From this network, a total of 106 fusion gene domain architectures utilized domain architectures only
344 found from their parent genes to form unique complete domain fusion families (Fig. S13B). The large
345 connected component within the network suggests several domain architectures are highly recurrent
346 across either parent genes or the final fusion and span multiple fusion families. Importantly, while most
347 parent genes have domains, many of the fusion genes did not involve any of the domains from at least one
348 parent gene (Fig. S13B-D). Without a domain from one of the parent genes, a novel domain architecture
349 was not produced, which would explain the large fraction of fusion genes that led to no change in the
350 n-gram networks across the TCGA cohorts (Fig. 5B). Next, we identified domain n-grams that either 1)
351 generate a large fraction of novel domain architecture or 2) display a propensity to be donated by either
352 the 5' or 3' parent genes. We find domains such as the KRAB domain and Paired domain are frequently
353 donated by the 5' parent, while the homeobox domain (HD) is donated by the 3' gene. However, most
354 fusions involving the KRAB or HD domains frequently have no domains donated from the other partner
355 gene, resulting in a fusion with only the KRAB or HD domain. If the fusion gene partner for the KRAB
356 containing proteins does donate a domain, it results in a novel domain architecture. Meanwhile, some
357 domains like the Paired domain only result in novel domain architectures (Fig. 5D). When analyzing
358 fusions containing the Znf-C2H2 or protein kinase domains given their importance in the natural
359 proteome, we find each had at least 50% of fusion result in novel domain architectures. However, when
360 we analyze fusions with the GPCR-Rhodpsn-7TM domain, which is found in >600 proteins in the
361 proteome, but does not appear to have a critical role in the n-gram network architecture (Fig. 1I), we
362 find it only within seven fusion genes, and it rarely results in novel domain architectures. Altogether,
363 these results suggest that individual domains have an intrinsic property that determines their role within
364 generating gene fusions, which can be uncovered with these linguistic networks.

365 Individual domains can vary in the number of multiple domain partners[4, 7, 8] they combine with,
366 and our networks can identify this through centrality measurements. To determine if domains involved in
367 gene fusions were the promiscuous domains, we calculated the Gini-Simpson Diversity Index for these
368 domains within the natural proteome. For the diversity index, we calculated it for both the diversity of
369 domains that precede an individual n-gram and the domains that follow the n-gram. This allows us to
370 determine whether an n-gram has a propensity to have a diverse set of partners before or after it, and
371 relate it to whether the n-gram is donated primarily by the 5' (reflecting diversity indices for n-grams
372 following it), or the 3' (reflecting the preceding n-gram diversity index). For all n-grams within fusions
373 genes, the distribution of the diversity indices were skewed slightly higher than the rest of the proteome,
374 but this was not a defining characteristic of the top overall fusion n-grams (Fig. S14). However, for the
375 KRAB and Znf-C2H2 domains, their propensity to generate novel domain architectures may be related
376 to having multiple existing domain partners – as reflected in a high degree centrality – but being

377 comprised of one dominate n-gram, lowers their diversity index (Fig. 1I, S14B). Alternatively, the
378 GPCR-Rhodpsn-7TM domain suggests its propensity to not form novel domain architectures may be due
379 to having few other n-grams it connects, and having single n-gram dominate the collection of domains in
380 combines with and result in a diversity index close to 0 (Fig. 1I, S14B). Meanwhile, for the protein kinase
381 and HD domains, these trends with the diversity index could not explain their properties within fusion
382 gene domain architectures. Rather, their centrality measurements within the complete n-gram network
383 could help explain their involvement in both preexisting and novel domain architectures. However, when
384 plotting the novel domain architecture fraction against the centrality metrics for all n-grams within
385 fusion genes, we found no correlation (Fig. 5E). Altogether, our results further suggest that the fusion
386 gene domain architectures follow the principles regulating domain architecture development. Further, the
387 collection of properties including the diversity of domain partners and the involvement in connecting
388 obligate proteins can contextualize the grammatical rules for individual n-grams.

389 Kinase fusion have been frequently identified across most cancers[44] with the tyrosine kinase domain
390 specifically being overrepresented within gene fusions[42, 46, 47]. We wanted to understand whether
391 kinase fusions identified in our analysis differed if a kinase domain was related to the pTyr or pSer/Thr
392 system. We found similar numbers of both the pSer/Thr and pTyr kinase domains across all fusions and
393 both domain families generated the same fraction of novel domain architectures (Fig. S15A,C).
394 Constructing an n-gram network from these gene fusions only 20 n-grams were common to both kinase
395 fusion types and the most highly connected nodes within the network were either specific to pSer/Thr
396 kinases (AGC-kinase, C-terminal domain) or common to both (FN3, Ig subtype 2, or the PH domains)
397 (Fig. S15B-D). Collectively, these results suggest that kinase domains generally have intrinsic properties
398 that enable neofunctionalization through diverse domain combinations. This result further supports our
399 suggestion that the high centrality measurements of the kinase domain reflect its involvement across
400 biological functions by connecting distinct n-gram families.

401 Discussion

402 Here, we applied n-gram analysis with network approaches to characterize the protein domain and
403 multidomain landscape of the human proteome. Assembling the domain n-grams into networks agrees
404 with past findings, that a small fraction of domains combine with a diverse set of domain
405 partners[3, 7, 8] (Fig. 1, S1), but also highlights that about 300 multidomain architectures represent
406 single proteins or protein families (Fig. S2). About 95% of the human proteome contains up to 10
407 domains which allows for a 10-gram model to sufficiently recover the distribution of domain n-grams and
408 recreate a complete n-gram network that 2-gram networks cannot (Fig. 2). To understand the insights
409 n-gram networks can provide for individual signaling subsystems, we further investigated the different
410 phosphorylation systems. We found that the domains making up the pTyr system were unique in
411 generating a complete connected graph and that this property likely evolved during the origins of
412 metazoan species (Fig. 3, 4). Interestingly, the n-gram network topologies highlights how selective
413 pressures from evolution can generate specific n-grams to bridge different PTM system components such
414 as the SH2|SH2|PTP architecture, but represent a small fraction of the complete system. Further, this
415 evolutionary analysis suggests that each PTM system converges toward a common set of grammatical
416 rules, such as eraser domains being loosely connected to the rest of system, that reflects the evolutionary
417 age of the PTM system. Since cancer progression can represent a potentially active selection process that
418 can create novel domain architectures to expand the grammatical rules of the proteome, we analyzed the
419 gene fusions. We found few fusions connect domains with obligate functions that do share common
420 domain partners (Fig. 5), but certain domains such as the protein kinase domain are frequently found
421 within fusion genes (Fig. 5F). However, these fusions cannot easily predict patient survival outcomes.
422 Studying gene fusions highlight that the principles that determine feasible domain combinations from
423 evolution remain during cancer progression. Collectively, the results highlight the uses of domain
424 architectures to study molecular functions beyond predicting the evolution and functionality of protein
425 families. Further, these results highlight that our n-gram network analysis can uncover rules akin to
426 grammar that determine feasible domain combinations, which can complement existing protein-protein

427 interaction networks by abstracting the functional connections within signaling subnetworks.

428 We applied the n-gram network analysis to cancer fusion genes to understand the frequency and
429 types of novel domain architectures being generated. From this analysis we found that most predicted
430 fusion gene domain architectures result in preexisting n-grams agree and that novel domain architectures
431 primarily utilizes domains with common domain partners (Fig. 5), but rarity of gene fusions compared
432 to other somatic mutations[41–43] makes findings on changes in patient survival inconclusive (Figs. S10,
433 S11). Kinase fusions though represent one of the largest classes of gene fusions and have been widely
434 identified across a variety of cancers[42, 44], which our full pancancer n-gram network analysis
435 corroborated (Fig. 5F). One of the other major classes of frequent gene fusions are transcription factors
436 fusions, which when involved in gene fusions are suggested to exert dominant negative effects[46]. In our
437 analysis, only Pointed|ETS transcription factor domain architecture was one of the most common
438 domain n-grams in our dataset, but rarely generated novel domain architectures (Fig. S13C) nor
439 impacted n-gram network topology. This reflects the prevalence of ETS fusions especially through the
440 TMPRSS2-ERG fusion within prostate cancer[39, 48], but has limited correlations to clinical
441 outcomes[40, 49]. However, this in combination with our results on patient survival (Fig. S10, S11)
442 emphasize the complexity of interpreting the presence of gene fusion in patient prognosis. Few gene
443 fusions are considered to be putative drivers of disease[50], and results have suggested in some instances
444 gene fusions are passenger aberrations[45]. However, recent studies have identified chimeric mRNA
445 species predicted to generate fusion genes within disease-free tissues[51, 52], but the contributions of
446 these gene fusions to cancer development or prognosis remain unclear.

447 Interestingly, by incorporating evolutionary analysis of the n-gram networks for the pTyr and
448 pSer/Thr systems (Fig. 4), we uncovered a set of grammatical rules that each reversible PTM system
449 appears to converge towards. During the rapid expansion of the pTyr system, which established pTyr
450 residues as novel, orthogonal signaling currency[36, 53], species are sampling several configurations of the
451 rules that determine domain ordering. However, evolution still promotes a convergence of rules which
452 keep domains that act as "verbs" separate from one another, and loosely connect the eraser domains if at
453 all with the rest of the system. The pTyr system is not the only signaling system that recently evolved.
454 The KRAB domain, which was also identified across our analyses to exert some influence in the n-gram
455 network, recently evolved during the transition towards vertebrates[54] to counter the expansion of
456 transposable elements within mammalian genomes[55]. While the function of many KRAB containing
457 Zinc-finger proteins (KRAB-ZFPs) have not been widely characterized, their role in embryonic
458 development have been widely appreciated due to KRAB-ZFPs recruitment of KAP1 to modulate
459 chromatin states[56]. This rapid evolution, similar to the pTyr system, emphasize that domains and
460 their combinations not only encode the evolutionary jumps of protein families[5] but reflect changes in
461 the molecular ecosystems available to cells. However, our n-gram networks can uncover the guiding
462 grammatical rules of individual signaling subnetworks, and could be applied to further study and
463 understand KRAB-ZFPs and the wider transposable element regulatory system.

464 Our analysis has generated a computational framework for describing domain architectures using
465 both linguistics and network approaches. However, our analysis still is limited in describing the complete
466 domain landscape present within cells. We retrieved and analyzed only the canonical protein isoforms,
467 which can omit proteoforms of individual genes that arise due to alternative splicing that impact
468 protein-protein and domain-domain interactions[57]. However, alternative splicing infrequently impacts
469 domain architectures but when reported involves repetitive domains such as the Znf-C2H2 and Ig-like
470 domains[58]. Additionally, the continued improvement of protein structure algorithms like AlphaFold[16]
471 have led to an expansion of the predicted structural folds without known functions but still represent the
472 evolution of protein families[28, 59]. Altogether, these suggest the proteome continues to evolve through
473 various mechanisms. However, the computational framework we have described here is flexible towards
474 describing and characterizing the expanded proteome, which can be further supplemented by molecular
475 interaction or function annotations.

Materials and Methods

Retrieving UniProt IDs for the human proteome and post-translational modification

For the human proteome, UniProtKB IDs were retrieved using pybiomart to map between Ensembl gene IDs and reviewed UniProtKB IDs. For individual post-translational modification (PTM) systems, InterPro IDs for the different domains that make up the PTM system were retrieved using the IDs listed in Table S1 using the InterPro module of CoDIAC[24]. For analyzing the phosphorylation systems in all species except humans, mice (*Mus musculus*) and rats (*Rattus norvegicus*) both reviewed and unreviewed UniProt records were fetched. To ensure unreviewed UniProtKB records are not mapping to same gene within individual species, UniProt entries on the evidence level, cross references to Ensembl, the NCBI Gene, and RefSeq databases, protein length, and gene symbol were fetched to determine which record represented identified genes and full protein coding sequences. Reviewed records were given top priority followed by records with cross references to other databases. Records which mapped to the same cross reference IDs were then compared by protein existence levels and finally amino acid length sequence. For UniProtKB records which required comparing amino acid length sequences, the record with the longest length was retained. The complete list of species and strain names used during fetching is provided in Table S2.

Fetching InterPro protein domain architectures and generating domain n-grams.

To fetch protein domain architectures from InterPro, we utilized the UniProt module from our recently developed python package CoDIAC[24] by inputting fetched UniProtKB IDs into the UniProt module from CoDIAC. The resulting reference file contains all InterPro and UniProt domain architectures and reference sequences for each queried protein and was used for downstream analysis. All results were fetched using the 2024 September 4th build of the InterPro and UniProt databases. The retrieved protein domain architectures were then separated into n-grams of the length of interest for each n-gram model. For building the PTM System Domain Focused n-gram models, only n-grams that contained domains of interest were fetched from the complete protein domain architecture.

Measuring n-gram model information gain and relative entropy.

N-gram models rely on the Markov assumption where the probability of a specific n-gram depends on the conditional probability of the next domain, d_n , given the preceding sequence of domains, d_{n-N+1} . This can be estimated for n-gram using the maximum likelihood estimate (MLE):

$$p_{MLE}(d_n|d_{n-N+1:n-1}) = \frac{C(d_{n+N-1:n-1}, d_n)}{C(d_{n+N-1:n-1})}$$

Where N represents the maximum length of n-grams being evaluated (i.e. N=2 for bigrams or N=5 for 5-grams). The counts of a specific n-gram ($d_{n+N-1:n-1}, d_n$) is represented by $C(d_{n+N-1:n-1}, d_n)$. These probabilities are then used to calculate the entropy of an n-gram model ($H_n(x)$) using Shannon's entropy:

$$H_n(x) = - \sum p(x) \log_2 p(x)$$

For individual domains the probabilities are given by the relative frequencies for each domain within the corpus of domain architectures. For longer n-grams, the entropy represents the sum of weighted probabilities which can be estimated by:

$$\begin{aligned} H_n(x) &= - \frac{1}{N_{ng}} \sum C(d_{n+N-1:n-1}) \log_2 \frac{C(d_{n+N-1:n-1}, d_n)}{C(d_{n+N-1:n-1})} \\ &= - \frac{1}{N_{ng}} \sum C(d_{n+N-1:n-1}) \log_2 p_{MLE}(d_n|d_{n+N-1:n-1}) \end{aligned}$$

Where N_{ng} represents the total number of n-grams with length N. The entropy of an n-gram model is then used to determine the relative information gain $I(x)$ from the unigram (only single domain

513 frequency distributions) model ($H_1(x)$):

$$I(x) = H_n(x) - H_1(x)$$

514 To compare how the distributions of n-grams change using different n-gram models we use the relative
515 entropy also known as the Kullback-Leibler divergence defined as:

$$D_{KL}(P||Q) = \sum P(X) \log_2 \frac{P(X)}{Q(X)}$$

516 Where $P(X)$ and $Q(X)$ represent the probability distributions within both n-gram models and $Q(X)$ is
517 the baseline model that contains all n-grams within $P(X)$.

518 **Calculating network centrality measurements.** For nodes within the largest connected
519 component, the betweenness and degree centrality measurements were calculated as implemented in the
520 networkx python package. Degree centrality is defined as the total fraction of all nodes connected to
521 node v . The betweenness centrality measurement of node v is the sum of fractions of pairwise shortest
522 paths that pass through node v , which is defined as:

$$c_B(v) = \sum_{s,t \in V} \frac{\sigma(s,t|v)}{\sigma(s,t)}$$

523 Where V is the set of nodes, $\sigma(s,t)$ represents the number of shortest paths between nodes s and t , while
524 $\sigma(s,t|v)$ represents the number of shortest paths that go through node v .

525 **Predicting domain architectures for gene fusions.** Genomic breakpoints for gene fusions were
526 retrieved from the ChimerDB[39] for the TCGA cohort. Fusions that were mapped to the current human
527 genome build (hg38), predicted to be in-frame, and were designated as found within the ChimerSeq+
528 dataset representing high confidence fusions were selected for further analysis (5579 total fusions).
529 Genomic breakpoints were then retrieved for each parent gene and mapped to exon and the protein
530 coding sequence positions. The base pair position was then translated to an amino acid position and
531 used to determine which domains were donated towards the fusion gene (Fig. S9). Domains which were
532 truncated by the breakpoint location were not included in the final predicted domain architecture.

533 **Calculating Gini-Simpson Diversity Index for domain n-grams.** For n-grams of with a length
534 of 10 or less, for each domain n-gram of interest d_n all $n+1$ n-grams containing the n-gram were
535 retrieved. The set of domain n-grams were then split into n-grams where d_n started or ended the n-gram.
536 For the n-grams starting with d_n were used to calculate the diversity index for following n-grams, while
537 those ended were used for the diversity index of preceding n-grams. The diversity index was calculated
538 using the Gini-Simpson Diversity Index as defined for small datasets:

$$D = 1 - l = 1 - \frac{\sum_{i=1}^R n_i(n_i - 1)}{N(N - 1)}$$

539 Where R is the collection of $n+1$ domain n-grams, N is the total count of the n-grams in the set, and n_i
540 is the count for each individual domain n-gram.

541 **Species N-gram Similarity Index** For comparing the n-grams of the pTyr and pSer/Thr systems
542 between individual species, the Jaccard similarity index, J , was calculated using:

$$J(A, B) = \frac{|A \cap B|}{|A \cup B|}$$

543 Where A and B represent the sets of domain n-grams found within individual species.

544 **TCGA Patient Survival Analysis.** Clinical attributes for the TCGA study cohorts were retrieved
545 from cBioPortal[60]. For univariate patient survival analysis, patients were stratified on if a tumor
546 harbored one or multiple of the fusion genes within our analyzed fusion gene dataset. Patients with
547 single fusions were then further stratified based on the n-gram network impacts caused by the fusion
548 gene (Fig. 5A). Statistically significant changes in survival probabilities were determined by using
549 pairwise log-rank tests as implemented in the lifelines python package.

550 Acknowledgments

551 We would like to acknowledge the constructive and critical assessment of the presented work from the
552 entire Naegle lab. The authors thank Bruce Mayer for helpful discussions about the phosphotyrosine
553 system of *Monosiga brevicollis*. This work was supported by funding from the National Institute of
554 General Medical Sciences (5R35GM138127).

References

1. Mayer BJ (2015) The discovery of modular binding domains: building blocks of cell signalling. *Nat Rev Mol Cell Biol* 16(11):691–8.
2. Moore AD, Björklund AK, Ekman D, Bornberg-Bauer E, Elofsson A (2008) Arrangements in the modular evolution of proteins. *Trends Biochem Sci* 33(9):444–51.
3. Ekman D, Björklund AK, Elofsson A (2007) Quantification of the elevated rate of domain rearrangements in metazoa. *J Mol Biol* 372(5):1337–48.
4. Han JH, Batey S, Nickson AA, Teichmann SA, Clarke J (2007) The folding and evolution of multidomain proteins. *Nat Rev Mol Cell Biol* 8(4):319–30.
5. Jin J, et al. (2009) Eukaryotic protein domains as functional units of cellular evolution. *Science Signaling* 2(98).
6. Buljan M, Bateman A (2009) The evolution of protein domain families. *Biochem Soc Trans* 37(Pt 4):751–5.
7. Apic G, Huber W, Teichmann SA (2003) Multi-domain protein families and domain pairs: comparison with known structures and a random model of domain recombination. *Journal of Structural and Functional Genomics* 4(2/3):67–78.
8. Basu MK, Carmel L, Rogozin IB, Koonin EV (2008) Evolution of protein domain promiscuity in eukaryotes. *Genome Research* 18(3):449–461.
9. Basu MK, Poliakov E, Rogozin IB (2008) Domain mobility in proteins: functional and evolutionary implications. *Briefings in Bioinformatics* 10(3):205–216.
10. Yu L, et al. (2019) Grammar of protein domain architectures. *Proceedings of the National Academy of Sciences* 116(9):3636–3645.
11. Hayete B, Bienkowska JR (2005) Gotrees: predicting go associations from protein domain composition using decision trees. *Pac Symp Biocomput* pp. 127–38.
12. Chou KC, Cai YD (2002) Using functional domain composition and support vector machines for prediction of protein subcellular location. *J Biol Chem* 277(48):45765–9.
13. Ofer D, Brandes N, Linial M (2021) The language of proteins: Nlp, machine learning & protein sequences. *Comput Struct Biotechnol J* 19:1750–1758.
14. Bepler T, Berger B (2021) Learning the protein language: Evolution, structure, and function. *Cell Systems* 12(6):654–669.e3.
15. Lin Z, et al. (2023) Evolutionary-scale prediction of atomic-level protein structure with a language model. *Science* 379(6637):1123–1130.
16. Jumper J, et al. (2021) Highly accurate protein structure prediction with alphafold. *Nature* 596(7873):583–589.
17. Scaiewicz A, Levitt M (2015) The language of the protein universe. *Curr Opin Genet Dev* 35:50–6.
18. Errington WJ, Bruncsics B, Sarkar CA (2019) Mechanisms of noncanonical binding dynamics in multivalent protein-protein interactions. *Proc Natl Acad Sci U S A* 116(51):25659–25667.
19. Mayer BJ, Hirai H, Sakai R (1995) Evidence that sh2 domains promote processive phosphorylation by protein-tyrosine kinases. *Curr Biol* 5(3):296–305.

20. Wang M, Kurland CG, Caetano-Anollés G (2011) Reductive evolution of proteomes and protein structures. *Proc Natl Acad Sci U S A* 108(29):11954–8.
21. Vogel C, Berzuini C, Bashton M, Gough J, Teichmann SA (2004) Supra-domains: evolutionary units larger than single protein domains. *J Mol Biol* 336(3):809–23.
22. Luck K, et al. (2020) A reference map of the human binary protein interactome. *Nature* 580(7803):402–408.
23. Peng X, Wang J, Peng W, Wu FX, Pan Y (2017) Protein-protein interactions: detection, reliability assessment and applications. *Brief Bioinform* 18(5):798–819.
24. Kandoor A, et al. (2024) Codiac: A comprehensive approach for interaction analysis reveals novel insights into sh2 domain function and regulation. *bioRxiv* p. 2024.07.18.604100.
25. Paysan-Lafosse T, et al. (2023) Interpro in 2022. *Nucleic Acids Res* 51(D1):D418–D427.
26. Mistry J, et al. (2021) Pfam: The protein families database in 2021. *Nucleic Acids Res* 49(D1):D412–D419.
27. Letunic I, Khedkar S, Bork P (2021) Smart: recent updates, new developments and status in 2020. *Nucleic Acids Res* 49(D1):D458–D460.
28. Waman VP, et al. (2024) Cath 2024: Cath-alphaflow doubles the number of structures in cath and reveals nearly 200 new folds. *J Mol Biol* 436(17):168551.
29. Urrutia R (2003) Krab-containing zinc-finger repressor proteins. *Genome Biol* 4(10):231.
30. Rosspopoff O, Trono D (2023) Take a walk on the krab side. *Trends in Genetics* 39(11):844–857.
31. Najafabadi HS, et al. (2015) C2h2 zinc finger proteins greatly expand the human regulatory lexicon. *Nat Biotechnol* 33(5):555–62.
32. Schmitges FW, et al. (2016) Multiparameter functional diversity of human c2h2 zinc finger proteins. *Genome Res* 26(12):1742–1752.
33. Needham EJ, Parker BL, Burykin T, James DE, Humphrey SJ (2019) Illuminating the dark phosphoproteome. *Science Signaling* 12(565).
34. Hunter T (2012) Why nature chose phosphate to modify proteins. *Philos Trans R Soc Lond B Biol Sci* 367(1602):2513–6.
35. Pincus D, Letunic I, Bork P, Lim WA (2008) Evolution of the phospho-tyrosine signaling machinery in premetazoan lineages. *Proc Natl Acad Sci U S A* 105(28):9680–4.
36. Lim WA, Pawson T (2010) Phosphotyrosine signaling: evolving a new cellular communication system. *Cell* 142(5):661–7.
37. Machida K, et al. (2007) High-throughput phosphotyrosine profiling using sh2 domains. *Mol Cell* 26(6):899–915.
38. Costa R, et al. (2016) Fgfr3-tacc3 fusion in solid tumors: mini review. *Oncotarget* 7(34):55924–55938.
39. Jang YE, et al. (2020) Chimerdb 4.0: an updated and expanded database of fusion genes. *Nucleic Acids Res* 48(D1):D817–D824.
40. Pettersson A, et al. (2012) The tmprss2:erg rearrangement, erg expression, and prostate cancer outcomes: a cohort study and meta-analysis. *Cancer Epidemiol Biomarkers Prev* 21(9):1497–509.

41. Mitelman F, Johansson B, Mertens F (2004) Fusion genes and rearranged genes as a linear function of chromosome aberrations in cancer. *Nat Genet* 36(4):331–4.
42. Latysheva NS, Babu MM (2016) Discovering and understanding oncogenic gene fusions through data intensive computational approaches. *Nucleic Acids Res* 44(10):4487–503.
43. Forbes SA, et al. (2017) Cosmic: somatic cancer genetics at high-resolution. *Nucleic Acids Res* 45(D1):D777–D783.
44. Stransky N, Cerami E, Schalm S, Kim JL, Lengauer C (2014) The landscape of kinase fusions in cancer. *Nat Commun* 5:4846.
45. Kalyana-Sundaram S, et al. (2012) Gene fusions associated with recurrent amplicons represent a class of passenger aberrations in breast cancer. *Neoplasia* 14(8):702–8.
46. Frenkel-Morgenstern M, Valencia A (2012) Novel domain combinations in proteins encoded by chimeric transcripts. *Bioinformatics* 28(12):i67–74.
47. Ortiz de Mendíbil I, Vizmanos JL, Novo FJ (2009) Signatures of selection in fusion transcripts resulting from chromosomal translocations in human cancer. *PLoS One* 4(3):e4805.
48. Kumar-Sinha C, Tomlins SA, Chinnaiyan AM (2008) Recurrent gene fusions in prostate cancer. *Nat Rev Cancer* 8(7):497–511.
49. Esgueva R, et al. (2010) Prevalence of *tmprss2-erg* and *slc45a3-erg* gene fusions in a large prostatectomy cohort. *Mod Pathol* 23(4):539–46.
50. Mertens F, Johansson B, Fioretos T, Mitelman F (2015) The emerging complexity of gene fusions in cancer. *Nat Rev Cancer* 15(6):371–81.
51. Singh S, et al. (2020) The landscape of chimeric rnas in non-diseased tissues and cells. *Nucleic Acids Res* 48(4):1764–1778.
52. Babiceanu M, et al. (2016) Recurrent chimeric fusion rnas in non-cancer tissues and cells. *Nucleic Acids Res* 44(6):2859–72.
53. Liu BA, et al. (2011) The sh2 domain-containing proteins in 21 species establish the provenance and scope of phosphotyrosine signaling in eukaryotes. *Sci Signal* 4(202):ra83.
54. Imbeault M, Helleboid PY, Trono D (2017) Krab zinc-finger proteins contribute to the evolution of gene regulatory networks. *Nature* 543(7646):550–554.
55. Rosspopoff O, Trono D (2024) Take a walk on the krab side: (trends in genetics, 39:11 p:844-857, 2023). *Trends Genet* 40(2):203–205.
56. Senft AD, Macfarlan TS (2021) Transposable elements shape the evolution of mammalian development. *Nat Rev Genet* 22(11):691–711.
57. Yang X, et al. (2016) Widespread expansion of protein interaction capabilities by alternative splicing. *Cell* 164(4):805–17.
58. Light S, Elofsson A (2013) The impact of splicing on protein domain architecture. *Curr Opin Struct Biol* 23(3):451–8.
59. Schaeffer RD, et al. (2023) Classification of domains in predicted structures of the human proteome. *Proc Natl Acad Sci U S A* 120(12):e2214069120.
60. Cerami E, et al. (2012) The cbio cancer genomics portal: an open platform for exploring multidimensional cancer genomics data. *Cancer Discov* 2(5):401–4.